A Novel DGS-Based Bandstop Filters Integrated Compact Four-Port MIMO Antenna for IEEE 802.11n/ac WLAN Standards

Kabir Das Ayinala
Dept. of Electrical Engineering
National Institute of Technology Rourkela,
Rourkela, India
518ee7017@nitrkl.ac.in

Prasanna Kumar Sahu
Dept. of Electrical Engineering
National Institute of Technology Rourkela,
Rourkela, India
pksahu@nitrkl.ac.in

***Abstract* — This work introduces a compact novel four-port Multiple-Input Multiple-Output structure with DGS-based decoupling elements for the 5.2 GHz band of WLAN standards. The DGS decoupling elements are L-shaped open-ended slots etched on the ring-shaped common ground plane between the curve-shaped radiating elements. The optimized decoupling slots function as bandstop filters to suppress the surface current distribution through the common ground plane in the targeted 5.2 GHz band (5.15 – 5.35 GHz) to enhance the isolation. The MIMO antenna achieves peak isolation of 23 and 26 dB between adjacent and diagonal elements despite its compact footprint of 24 × 24 mm².**

Keywords — compact, defective ground structure, isolation, MIMO, wireless LAN

I. INTRODUCTION

In the current wireless scenario, compact ultra-high-speed wireless devices are the most attractive gadgets to meet the requirements of modern wireless applications. To support enhanced data rates, the most widely used WLAN standards IEEE 802.11n/ac are integrated with Multiple-Input Multiple-Output (MIMO) technology [1]. Moreover, these standards provide four to eight independent data streams [2]. This requirement grabs the attention of antenna designers to realize compact four-element MIMO structures. However, smaller element-to-element spacing of compact MIMO designs leads to strong mutual interaction between the elements. This mutual interaction (poor isolation) degrades the diversity/MIMO performance. Hence, implementing compact quad-element MIMO configurations with higher decoupling levels is essential for space-constrained wireless devices.

Several techniques have been proposed in the literature to enhance the decoupling level and thereby diversity/MIMO performance. Metamaterial-based filter in [3] and fractal-shaped electromagnetic bandgap immaterial in [4] provide isolation below 15 and 24.67 dB, respectively. However, these decoupling structures are introduced for dual-element MIMO structures. In [5], polarization diversity is explored between the double-side curve-shaped monopole radiators to decouple the elements to 13 dB. The ring-shaped metal strips in [6] reported a minimum isolation level of 17 dB in the accomplished band of 2.3 – 2.7 GHz. In [7], parasitic elements of thin metal strips are considered to decouple the elements of the four-port MIMO configuration effectively. Furthermore, these quad-port MIMO designs [5-7] considered separate ground planes for the enhancement of isolation in addition to the applied isolation improvement techniques. However, using separate ground planes for multi-antenna systems is not practical as these may not ensure the same reference voltage levels over the multiple grounds. The consequences of these individual ground planes are well addressed by Mahammad S. Sharawi in [8].

The MIMO designs in [9-11] are introduced with the common ground planes. In [9], pattern diversity is explored between the radiators of array topology-based monopole slots. It achieves isolation of more than 22 dB with relatively large size of $1.0\lambda_0 \times 1.0\lambda_0$. The defective ground structure in [10] reported minimum isolation of 15.4 dB between the modified slot radiators. In [11], meander antenna elements with a ring-shaped common ground plane provide poor isolation of 10 dB.

The literature study shows that the realization of compact MIMO designs with reduced mutual coupling is challenging, particularly for the continuous ground plane configurations. In this work, DGS-based bandstop filters integrated ring-shaped continuous ground plane compact four-port MIMO configuration is introduced for the 5.2 GHz band of WLAN. It has a small size of 24 × 24 mm² and is more compact than the similar designs reported earlier, as summarized in table 1. It achieves a minimum decoupling level of 15.5 dB across the targeted band 5.15 – 5.35 GHz, which is better than the similar design reported in [11] with a more compact structure. It provides very good radiation and diversity/MIMO characteristics over the operating band.

II. IMPLEMENTATION OF PRESENTED COMPACT FOUR-PORT MIMO CONFIGURATION

Fig. 1 displays the topology of the presented compact four-port MIMO design with its optimized dimensions. It has a compact area of $0.14\ \lambda_0^2$. It is implemented over an inexpensive FR-4 dielectric material (ϵ_r= 4.4 and $tan\delta$= 0.02) of thickness 0.8 mm. The MIMO antenna elements are indicated as #1, #2, #3, and #4, and their respective ports are denoted as P_1, P_2, P_3, and P_4. The integrated DGS-based decoupling elements function as bandstop filters (BSFs), designated as BSF-1 to BSF-4. The MIMO antenna is realized using a 3D EM simulator, Ansys HFSS Vs. 17.1. The design and analysis of the presented MIMO antenna are illustrated as follows.

TABLE 1. THE COMPARISON OF INTRODUCED FOUR-PORT MIMO DESIGN WITH SIMILAR MIMO DESIGNS.

Ref.	Impedance bandwidth (MHz)	Antenna size (λ_0^2)	Isolation (dB)	ECC	Peak Gain (dBi)	Decoupling Technique	Common Ground
[05]	560 (1.68-2.24 GHz)	0.20	> 13	< 0.01	3.0	Polarization Diversity	No
[16]	400 (2.30-2.70 GHz)	0.26	> 17	< 0.04	3.7	Ring-shaped strips	No
[09]	1700 (4.50-6.20 GHz)	1.00	> 22	---	5.2	Pattern Diversity	Yes
[11]	1400 (5.30-6.70 GHz)	0.45	> 10	< 0.0004	4.0	Polarization Diversity	Yes
This work	**800 (4.90-5.7 GHz)**	**0.14**	> 15.5	< 0.0018	**4.12**	**DGS**	**Yes**

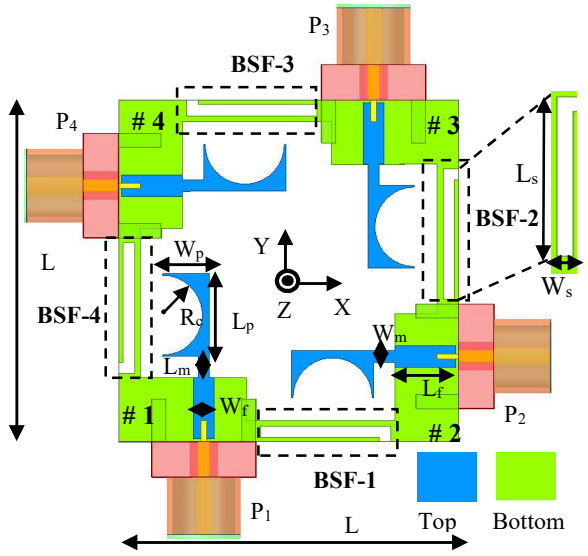

Fig.1. The geometry of the proposed compact MIMO design. Dimensions (mm): L=24, L_f= 4.5, W_f= 1.5 L_p=5.8, W_p=3.2, R_c=2.9, L_m=1.5, W_m=0.8, L_s=8.4, W_s=0.8.

The MIMO structure is implemented in two steps. Initially, in step-1, a four-port MIMO structure without decoupling elements is realized, as displayed in Fig.2(a), which is represented as Ant-1. It consists of four curve-shaped monopole radiators with partial ground planes that are inter-connected to obtain a ring-shaped common ground plane. The curve-shaped radiators are considered in the top layer as the curve shape facilitates miniaturization up to some extent. The continuous ground plane (bottom layer) avoids the limitations of separate ground planes discussed above and ensures the proper functioning of the MIMO system in practical scenarios. The antenna elements of the MIMO design are arranged perpendicular to each other to explore polarization diversity.

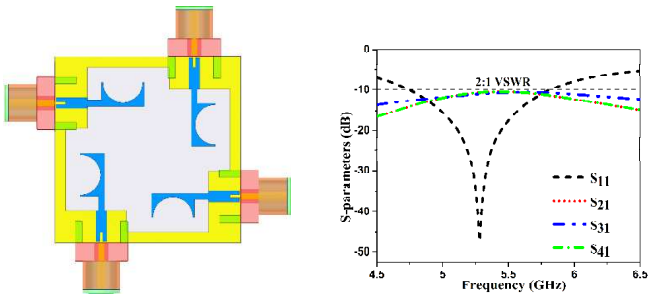

(a) (b)

Fig.2. (a) The geometry of Ant-1 (b) Its S-parameters.

The S-parameters of this presented MIMO geometry are shown in Fig. 2(b) when element #1 is excited with terminating others at 50-Ω matched loads. It shows the design resonates at 5.3 GHz and provides poor isolation of 10.5 dB among the antenna elements over the targeted band. The distributed current shown in Fig. 3 demonstrates that the high level of coupling between the elements is due to the propagation of surface current between the elements through the continuous ground plane. Furthermore, to confirm this, isolation characteristics of MIMO configuration with separate ground planes are compared with the Ant-1. The comparison shows the MIMO design without continuous ground plane reports an isolation improvement of 19 and 5 dB between the orthogonal and diagonal elements. This clearly shows, the poor isolation of Ant-1 is due to surface current propagation, and it needs to be suppressed by integrating a suitable decoupling structure.

As current propagation from the exciting antenna element to other elements is through the conducting metal strips between the antenna elements, to improve the isolation over the targeted band (5.15 – 5.35 GHz), a simple L-shaped quarter-wavelength open-ended slot-based structure is considered, as displayed in Fig. 4(a). The S-parameters reported in Fig. 4(b) demonstrate that the slot-based structure rejects the signal propagation to a maximum level of 27 dB at 5.3 GHz. That means the optimized slot functions as a bandstop filter to isolate port-1 and port-2 efficiently over the targeted bandwidth. The current distribution in Fig. 4(c) shows its principle of trapping EM energy across the bandstop filter at 5.3 GHz.

Now, in the 2nd step, the introduced compact MIMO structure designated as Ant-2 is implemented by etching the introduced slot-based bandstop filters on the continuous ground topology between the antenna elements, as depicted in Fig. 5(a).

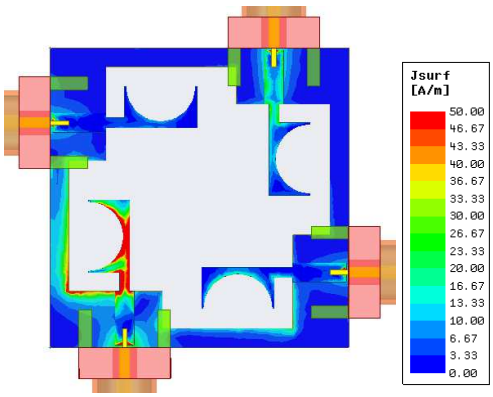

Fig. 3. The surface current distribution at 5.3 GHz

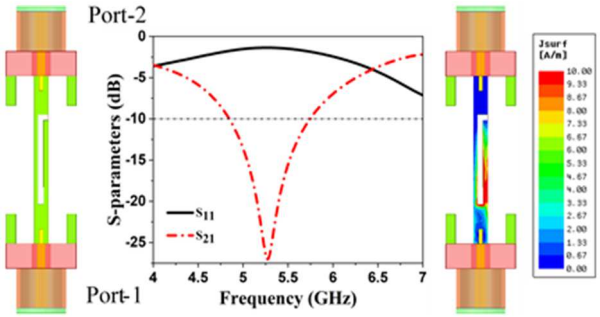

(a) (b) (c)

Fig. 4. (a) Schematic of microstrip band-stop filter (BSF) (b) S-parameters (c) Distributed current at 5.3 GHz.

As the decoupling slots are etched on the ground plane, these are referred to as defective ground structure bandstop filters (DGS-BSFs). The S- parameters of this proposed structure depicted in Fig. 5 (b) reports that the antenna accomplishes an impedance bandwidth of 800 MHZ (4.9 – 5.7 GHz), which covers the targeted 5.2 GHz band of WLAN. The decoupling level between the orthogonal and diagonal elements varies from 16 to 23 dB and 15.5 to 26 dB, respectively, over the 5.15 – 5.35 GHz frequency band. That means the integrated bandstop filter decoupling elements improve the isolation by 12.5 and 15 .5 dB between orthogonal and diagonal antenna elements compared to the MIMO structure without decoupling filters (Ant-1).

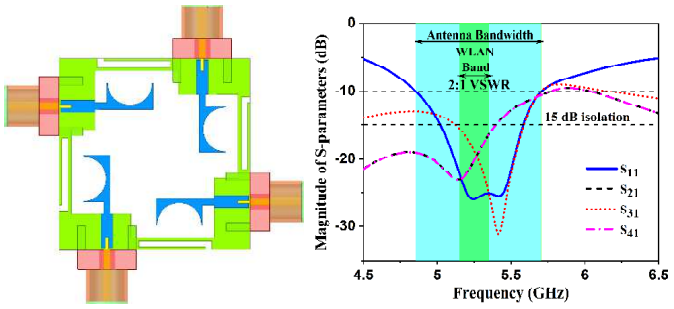

(a) (b)

Fig.5. (a) The geometry of proposed compact MIMO structure (b) Its simulated port parameters.

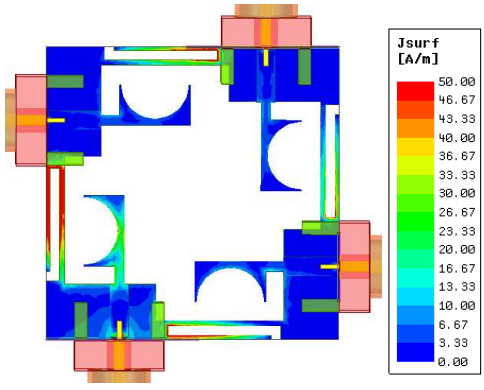

Fig. 6. The surface current distribution of Ant-B (proposed MIMO design) at 5.3 GHz when element #1 is excited.

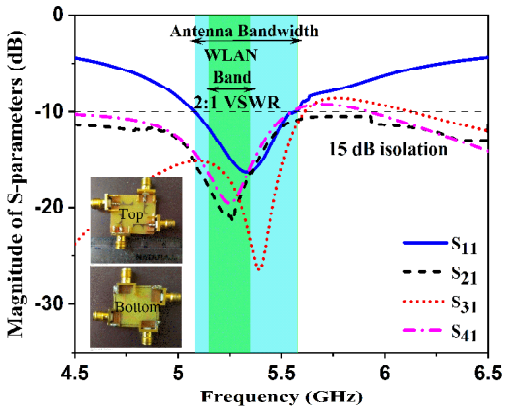

Fig. 7. Measured S-parameters of the presented MIMO structure.

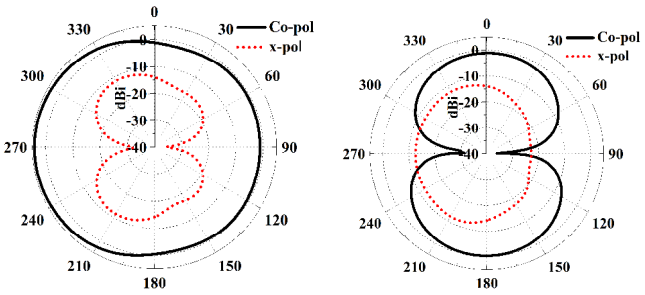

(a) (b)

Fig. 8. 2D radiation patterns of the proposed MIMO configuration at 5.3 GHz in (a) XZ-plane (H-plane) (b) YZ-plane (E-plane).

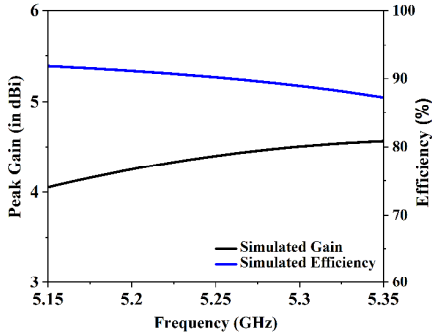

Fig. 9. Simulated peak gain and efficiency of the proposed antenna.

The improvement in decoupling level is demonstrated with the current distribution, as displayed in Fig. 6. When element #1 is powered, keeping others at the matched load, the bandstop filters effectively suppress the current propagation among the elements. The optimized presented quad-element simulation model is fabricated, and its port parameters are tested using Microwave Vector Network Analyzer (VNA). According to the measured S-parameters displayed in Fig. 7, the MIMO structure reports a bandwidth of 510 MHz (5.07 – 5.58 GHz) and a minimum decoupling level of 15.3 dB over the operating WLAN 5.2 GHz band.

The 2-D patterns of the presented MIMO antenna in the two orthogonal principal planes (H-plane and E-plane) are shown in Fig. 8. As reported in the plots, the patterns are almost omnidirectional and bidirectional in H (XZ) and E (YZ) planes. Furthermore, in both planes, the antenna maintains a decent co-pol to cross-pol difference. The peak gain and radiation

efficiency of the MIMO structure are plotted in Fig. 9. As reported, the proposed antenna reports a peak gain of more than 4.12 dBi and an efficiency of more than 88% over the 5.2 GHz WLAN frequency band of 5.15 – 5.35 GHz.

III. DIVERSITY PERFORMANCE

The MIMO antenna's diversity ability is validated with the Envelope Correlation Coefficient (ECC) and Total Active Reflection Coefficient (TARC) metrics. The ECC is the similarity index, which measures the similarity level between the signals received by the MIMO antenna elements. The MIMO antenna exhibits good diversity performance when the MIMO channels are highly independent of each other. The ECC is computed for isotropic/uniform wireless environments, using the following equation [7].

$$\rho_e(\mathrm{i},\mathrm{j}) = \frac{\left|\sum_{n=1}^{N} S_{\mathrm{i},n}^{*} S_{n,j}\right|^2}{\Pi_{k=i,j}\left[1-\sum_{n=1}^{N} S_{\mathrm{k},n}^{*} S_{n,\mathrm{k}}\right]} \quad (1)$$

Here i and j represent the variation of the number of elements from 1 to N. The plotted ECC values in Fig. 10 reported that the introduced MIMO antenna provides very good simulated/measured values of 0.0018/0.011, which are far below the standard value of 0.5 specified for the good diversity performance. Another important diversity metric, TARC, measures the impedance bandwidth more effectively than the normal reflection coefficient for multi-antenna systems, calculated using the equation specified below [11].

$$\Gamma_t^a = \frac{\sqrt{\sum_{i=1}^{N}|b_i|^2}}{\sqrt{\sum_{i=1}^{N}|a_i|^2}} \quad (2)$$

Here a_i and b_i are the input and output waves of multi-port systems. The antenna's simulated and measured TARC values depicted in Fig. 11 are below -10 dB for different excitation phase differences between the ports.

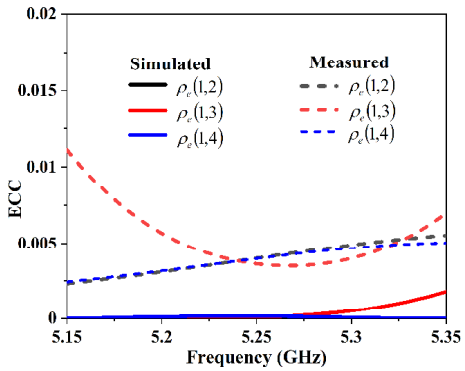

Fig.10. The ECC of the presented MIMO antenna.

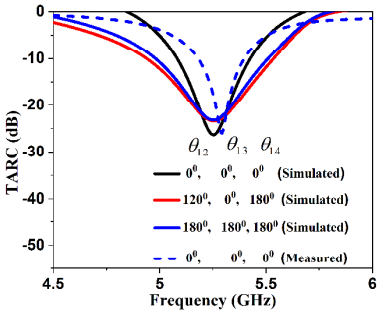

Fig.11. The TARC values of the presented MIMO antenna.

IV. CONCLUSION

This paper introduces a compact quad-element MIMO configuration with DGS-based bandstop filters integrated ring-shaped continuous ground plane for isolation enhancement. It has a smaller footprint of $0.38\lambda_0 \times 0.38\lambda_0$ and is more compact than the similar MIMO configurations reported in the literature. The proposed structure enhances the decoupling level by 12.5 and 15.5 dB compared to the MIMO structure without decoupling filters over the WLAN application's 5.2 GHz band (5.15 – 5.35 GHz). It provides excellent radiation characteristics with a very good diversity ability estimated in terms of its performance metrics ECC (<0.0018) and TARC (<-10 dB). The introduced MIMO configuration with compactness, common ground plane, and excellent performance is highly suitable for the IEEE 802.11n/ac standards enabled portable wireless devices.

REFERENCES

[1] M. A. Jensen and J. W. Wallace, "A review of antennas and propagation for MIMO wireless communications," *IEEE Trans. Antennas Propag.*, vol. 52, no. 11, pp. 2810–2824, 2004.

[2] O. Bejarano and E. W. Knightly, "IEEE 802.11ac: From channelization to multi-user MIMO," *IEEE Commun. Mag.*, vol. 51, no. 10, pp. 84–90, 2013.

[3] S. R. Thummaluru and R. K. Chaudhary, "Mu-negative metamaterial filter-based isolation technique for MIMO antennas," *Electron. Lett.*, vol. 53, no. 10, pp. 644–646, 2017.

[4] K. Sharma and G. P. Pandey, "Two port compact mimo antenna for ism band applications," *Prog. Electromagn. Res. C*, vol. 100, no. March, pp. 173–185, 2020.

[5] L. Malviya and K. Machavaram, "A low profile planar MIMO antenna with polarization diversity for LTE," no. December, 2017.

[6] A. A. Yussuf and S. Paker, "Design of a compact quad-radiating element MIMO antenna for LTE/Wi-Fi application," *AEU - Int. J. Electron. Commun.*, vol. 111, p. 152893, 2019.

[7] X. Tan, W. Wang, Y. Wu, Y. Liu, A. A. Kishk, and H. Wang, "Enhancing isolation and bandwidth in planar monopole multiple antennas using thin inductive line resonator," *AEU - Int. J. Electron. Commun.*, vol. 117, 2020.

[8] M. S. Sharawi, "Current Misuses and Future Prospects for Printed Multiple-Input, Multiple-Output Antenna Systems [Wireless Corner]," *IEEE Antennas Propag. Mag.*, vol. 59, no. 2, pp. 162–170, 2017.

[9] H.-T. Hu, F.-C. Chen, and Q.-X. Chu, "A compact directional slot antenna and its application in MIMO array," *IEEE Trans. Antennas Propag.*, vol. 64, no. 12, pp. 5513–5517, 2016.

[10] S. Pandit, A. Mohan, and P. Ray, "A compact four-element MIMO antenna for WLAN applications," *Microw. Opt. Technol. Lett.*, vol. 60, no. 2, pp. 289–295, 2018.

[11] S. Chouhan, D. K. Panda, M. Gupta, and S. Singhal, "Meander line MIMO antenna for 5.8 GHz WLAN application," *Int. J. RF Microw. Comput. Eng.*, vol. 28, no. 4, 2018.